Impact of *Fabp1/Scp-2/Scp-x* gene ablation (TKO) on hepatic phytol metabolism in mice[S]

Stephen M. Storey,* Huan Huang,* Avery L. McIntosh,* Gregory G. Martin,* Ann B. Kier,[†] and Friedhelm Schroeder[1,*]

Departments of Physiology and Pharmacology* and Pathobiology,[†] Texas A&M Veterinary Medical Center, Texas A&M University, College Station, TX 77843

ORCID IDs: 0000-0001-6741-2470 (S.M.S.); 0000-0001-5392-2947 (H.H.); 0000-0002-8663-8990 (A.L.M.); 0000-0002-0092-4612 (G.G.M.); 0000-0002-3545-7962 (F.S.)

Abstract **Studies in vitro have suggested that both sterol carrier protein-2/sterol carrier protein-x (*Scp-2/Scp-x*) and liver fatty acid binding protein [*Fabp1* (L-FABP)] gene products facilitate hepatic uptake and metabolism of lipotoxic dietary phytol. However, interpretation of physiological function in mice singly gene ablated in the *Scp-2/Scp-x* has been complicated by concomitant upregulation of FABP1. The work presented herein provides several novel insights: *i*) An 8-anilino-1-naphthalenesulfonic acid displacement assay showed that neither SCP-2 nor L-FABP bound phytol, but both had high affinity for its metabolite, phytanic acid; *ii*) GC-MS studies with phytol-fed WT and *Fabp1/Scp-2/SCP-x* gene ablated [triple KO (TKO)] mice showed that TKO exacerbated hepatic accumulation of phytol metabolites in vivo in females and less so in males. Concomitantly, dietary phytol increased hepatic levels of total long-chain fatty acids (LCFAs) in both male and female WT and TKO mice. Moreover, in both WT and TKO female mice, dietary phytol increased hepatic ratios of saturated/unsaturated and polyunsaturated/monounsaturated LCFAs, while decreasing the peroxidizability index. However, in male mice, dietary phytol selectively increased the saturated/unsaturated ratio only in TKO mice, while decreasing the peroxidizability index in both WT and TKO mice. These findings suggested that: *1*) SCP-2 and FABP1 both facilitated phytol metabolism after its conversion to phytanic acid; and *2*) SCP-2/SCP-x had a greater impact on hepatic phytol metabolism than FABP1.—** Storey, S. M., H. Huang, A. L. McIntosh, G. G. Martin, A. B. Kier, and F. Schroeder. **Impact of *Fabp1/Scp-2/Scp-x* gene ablation (TKO) on hepatic phytol metabolism in mice. *J. Lipid Res.* 2017.** 58: **1153–1165.**

Supplementary key words fatty acid binding protein 1/sterol carrier protein-2/sterol carrier protein-x • triple knockout • peroxisomal oxidation

Phytol, present in ruminant fat and milk products, is a branched-chain fatty alcohol derived via side-chain cleavage of chlorophyll by ruminant bacteria (1, 2). Defects in phytol metabolism result in accumulation of lipotoxic phytol metabolites (phytanic acid, pristanic acid) that is associated with Refsum's disease and other peroxisomal enzyme deficiency diseases in humans (3, 4). Hence considerable interest has focused on resolving the enzyme pathway and subcellular organelles wherein phytol undergoes hepatic metabolism/detoxification (1, 2, 5–7). Briefly, dietary phytol is transported by lipoproteins from the intestine to the liver where it is taken up, converted to phytanic acid in the endoplasmic reticulum, and then transported to the peroxisomal membrane for conversion to phytanoyl-CoA and internalization into the peroxisomal matrix. Within peroxisomes, phytanoyl-CoA undergoes several cycles of α- and β-oxidation followed by transfer of the resultant short-chain nonbranched product to mitochondria for completion of β-oxidation. Poorly soluble amphipathic lipids, such as phytol (and its metabolites, phytanic acid and phytanoyl-CoA), are highly membrane associated in aqueous environments and thus require protein "chaperone(s)" for transport through the cytosol to the endoplasmic reticulum (for conversion to phytanic acid) and from there to peroxisomes for further metabolism (8). While an intracellular phytol binding/transport protein serving the former function is as yet unresolved, several studies have suggested that the hepatic sterol carrier protein-2/sterol carrier protein-x (*Scp-2/Scp-x*) and liver fatty acid binding protein [*Fabp1* (L-FABP)] genes are candidates coding for the

This work was supported in part by the United States Public Health Service, National Institute of Diabetes and Digestive and Kidney Diseases Grant R01DK41402 (F.S. and A.B.K.).

Manuscript received 1 February 2017 and in revised form 7 April 2017.

Published, JLR Papers in Press, April 14, 2017
DOI https://doi.org/10.1194/jlr.M075457

Abbreviations: ANS, 8-anilino-1-naphthalenesulfonic acid; FABP1, liver fatty acid binding protein (L-FABP); FAME, fatty acid methyl ester; LCFA, long-chain fatty acid; 15:0-ME, 15:0-methyl ester, NAFLD, nonalcoholic fatty liver disease; SCP-2, sterol carrier protein-2; SCP-x, sterol carrier protein-x; TKO, *Fabp1/Scp-2/Scp-x* triple gene ablated mice (triple KO).

[1] To whom correspondence should be addressed.
e-mail: fschroeder@cvm.tamu.edu

[S] The online version of this article (available at http://www.jlr.org) contains a supplement.

respective proteins facilitating transport of phytol metabolites (e.g., phytanic acid, pristanic acid) through the cytosol and peroxisomal matrix.

Although nearly half of SCP-2 is highly localized in peroxisomes, the remainder is extraperoxisomal within cytosol (9–11). Some cytosolic SCP-2 is associated with two key transmembrane receptors localized within plasma membrane cholesterol-rich microdomains: *i*) caveolin-1, involved in long-chain fatty acid (LCFA) uptake and cell signaling (12–14); and *ii*) scavenger receptor B-1 (SRB1), which mediates uptake of another branched-side chain lipid (cholesterol) from HDL (15–18). Within peroxisomes, SCP-2 directly interacts with oxidative enzymes and stimulates phytanoyl-CoA 2-hydroxylase, the essential enzyme mediating the first step in peroxisomal α-oxidation of branched-chain fatty acids (8, 19). SCP-2 binds several phytol metabolites, including phytanic acid (formed at the endoplasmic reticulum) and phytanoyl-CoA (formed at the peroxisome), as well as pristanic acid, phytenic acid, and pristanoyl-CoA (formed within the peroxisomal matrix) (20, 21). Through an alternate transcription site, the *Scp-2/Scp-x* gene also produces SCP-x, an exclusively peroxisomal protein that is the only known branched-chain 3-ketoacyl-CoA thiolase (10, 22–24).

The other major hepatic protein potentially contributing to cytosolic binding/transport of branched-chain fatty acids within hepatocytes is the liver fatty acid binding protein (FABP1) (23, 25–27). FABP1 is highly localized in hepatocyte cytosol (200–400 μM in mice and several fold-higher in humans, levels that are 6- to 8-fold higher than those of SCP-2) (24, 28–30). Cytosolic FABP1 directly interacts with fatty acid transport protein-5 (FATP-5), localized within cholesterol-rich microdomains of the hepatocyte plasma membrane, where it is postulated to facilitate fatty acid uptake across the plasma membrane into the hepatocyte (31). Importantly, cytosolic FABP1 binds the first phytol metabolite (i.e., phytanic acid) formed at the endoplasmic reticulum (20, 32, 33). Although FABP1 also binds pristanic acid and phytenic acid, these metabolites are formed within the peroxisomal matrix, wherein, with some exception (34), FABP1 has not been localized (20, 32, 33).

Taken together, the above findings suggest that FABP1 may function primarily within cytosol to transfer phytanic acid from the endoplasmic reticulum to peroxisomes for intraperoxisomal transport and metabolism mediated by SCP-2 and SCP-x. Consistent with this possibility, overexpression of SCP-2, SCP-x, or FABP1 enhanced [^{3}H]phytanic acid uptake and oxidation in transfected L-cell fibroblasts (23, 35). Conversely, Fabp1 gene ablation inhibited [^{3}H]phytanic acid uptake and oxidation in mouse hepatocytes (26). Studies of the in vivo roles of these proteins in hepatic phytol metabolism are more difficult to interpret because expected reductions in phytol metabolism in *Scp-2/Scp-x*-null (17, 21, 36) or *Scp-x*-null (24) mice are complicated by concomitant compensatory several-fold upregulation of FABP1, as well as sex-differences in hepatic expression of these proteins.

To further address the roles of SCP-2/SCP-x and FABP1 in phytol metabolism and the sexual divergence in phytol oxidative pathways in a physiological context, the present study examined the impact of *Fabp1/Scp-2/Scp-x* gene ablation on hepatic phytol metabolism, as well as total fatty acid content in both male and female mice fed control diet versus a 0.5% phytol diet. The data showed that, although neither SCP-2 nor FABP1 bound phytol, both bound phytanic acid. Furthermore, triple KO (TKO) markedly impaired hepatic phytol metabolism and altered total fatty acid content (mass) and profile (composition) in a sex-dependent fashion. The data suggested a greater role for: *i*) FABP1 in transport of the primary phytol metabolite (i.e., phytanic acid) from the endoplasmic reticulum to peroxisomes; and *ii*) SCP-2 and SCP-x in intraperoxisomal transport of phytanoyl-CoA and/or subsequent metabolites to oxidative enzymes within the peroxisomal matrix.

MATERIALS AND METHODS

Materials

Fatty acid standards were purchased from Nu-Chek Prep, Inc. (Elysian, MN), methyl pristanate from Larodan AB (Malmo, Sweden), and phytol, phytanic acid, and phytanic methyl ester from Sigma-Aldrich (St. Louis, MO). The 8-anilino-1-naphthalenesulfonic acid (ANS) was obtained from Life Technologies (Grand Island, NY). Recombinant murine FABP1 (37, 38) and recombinant human SCP-2 (9, 39, 40) were isolated, delipidated, and the purity determined as described in the cited articles. All reagents and solvents used were of the highest grade available and cell culture tested. All glassware was washed with sulfuric acid-chromate before use.

Phytanic acid and phytol binding to FABP1 and SCP-2

Phytanic acid and phytol binding to FABP1 and SCP-2 was determined by ANS fluorescence displacement assay, as described (41). ANS is very weakly fluorescent in buffer and its fluorescence increase upon binding to FABP1 or SCP-2 was recorded at 24°C by scanning emission from 410 to 600 nm with 380 nm excitation using a Varian Cary Eclipse fluorescence spectrophotometer (Varian, Inc., Palo Alto, CA). First, FABP1 or SCP-2 (500 nM) was titrated with ANS (0–55 μM, forward titration). Second, in the reverse titration, ANS (100 nM) was titrated with an increasing amount of FABP1 (0–4 μM) or SCP-2 (0–30 μM). From the maximum of the reverse titration curve calculated by curve fitting, the fluorescence intensity of ANS (per nanomole) when fully bound to FABP1 or SCP-2 was calculated. This number was used in the forward titration to calculate the fractional saturation and free ANS concentration. K_d and B_{max} were calculated from the binding curve fractional saturation (Y) versus free ANS concentration (X). FABP1 and SCP-2 bound the synthetic fluorophore ANS with K_ds of 2.5 ± 0.2 μM and 9.4 ± 0.3 μM, respectively.

To determine phytanic acid and phytol binding affinity to FABP1 and SCP-2, samples of FABP1 or SCP-2 (500 nM) were preincubated with 35 or 50 μM ANS, respectively. Each was then titrated with phytanic acid (0–8 μM) or phytol (0–33 μM). The EC_{50} obtained from the displacement curve and the K_d for ANS were used to calculate K_i using the equation: $EC_{50}/[ANS] = K_i/K_d$.

Animal studies

Adult male and female (2 months of age, 20–30 g) inbred C57BL/6NCr WT mice were obtained from the Frederick Cancer Research and Development Center (Frederick, MD). Age- and sex-matched *Fabp1/Scp-2/Scp-x*-null [triple KO (TKO)] mice on

the C57BL/6NCr background (N6 backcross generation) were generated as previously described (42). Mice were given free access to water and food (standard rodent chow with 5% calories from fat) and kept on a 12 h light/12 h dark cycle. Mice in the facility were monitored quarterly for infectious diseases and were specific pathogen free, particularly in reference to mouse hepatitis virus. Animal protocols were approved by the Animal Care and Use Committee of Texas A&M University.

One week before the start of experiments, mice were switched to a modified AIN-76A rodent diet (5% calories from fat; diet D11243; Research Diets, Inc., New Brunswick, NJ). The modified AIN-76A rodent diet (control diet), essentially free of phytoestrogens and phytol, avoided potential diet-induced complications in gender comparisons (43, 44) and in fatty acid oxidation because phytol metabolites are, themselves, potent ligand activators of PPARα transcription of fatty acid oxidative enzymes (21, 33, 36, 45–47). After 1 week on the phytoestrogen-free phytol-free control diet, the mice were divided into two groups (eight female and eight male mice per group): one group remained on the control diet, while the other was switched to a modified AIN-76A rodent diet supplemented with 0.5% phytol (5% calories from fat; diet D01020601; Research Diets, Inc.). The mice were on the diets until they lost approximately 20% of their body weight. Due to the rapidity of weight loss by the TKO mice, the length of the study was 7 days. When lipids were extracted from both diets and assayed by GC-MS, as described below, phytanic acid was not detected, but a trace amount of phytol (0.058%) was present in the AIN-76A control diet. This was 8.5-fold less than in the 0.5% phytol-supplemented AIN-76A rodent control chow (diet D01020601; Research Diets, Inc.).

Body weight and food intake of all mice were monitored every other day. At the end of the study (day 7), animals were fasted overnight, anesthetized (100 mg/kg ketamine, 10 mg/kg xylazine), and cervical dislocation was used to ensure humane death. Livers were harvested, snap-frozen on dry ice, and stored at −80°C. For lipid extraction and fatty acid analysis, liver samples (∼0.1 g) were thoroughly minced, 0.5 ml PBS (pH 7.4) added, and homogenized with a motor-driven pestle (Tekmar Co, Cincinnati, OH) at 2,000 rpm. Protein concentration in the homogenate was determined by Bradford protein micro-assay (Bio-Rad, Hercules, CA) using Costar 96-well assay plates (Corning, Corning, NY) and quantitated with a BioTek Synergy 2 microplate reader (BioTek Instruments, Winooski, VT).

Liver lipid extraction and fatty acid methyl ester derivatization

Liver was homogenized as described above, an internal standard [15:0-methyl ester (15:0-ME)] added, lipids extracted with *n*-hexane:2-propanol (3:2, v/v) (48, 49), and the lipid extract divided into aliquots for fatty acid mass and composition determinations, which were stored under an atmosphere of N_2 to limit oxidation. Base-catalyzed transesterification (1 M KOH in methanol at 37°C for 20 min, reaction stopped with ethyl formate) was performed on aliquots of the extracted lipid fraction from each sample to convert the lipid acyl chains to fatty acid methyl esters (FAMEs). FAMEs were then extracted into petroleum ether, dried under N_2, and dissolved in *n*-hexane and again stored under an N_2 to limit oxidation. The protein extract residue was dried, digested overnight in 0.2 M KOH (50), and protein concentration determined by the method of Bradford (51).

Resolution and quantitation of liver FAMEs by GC and GC-MS

Individual FAME species were resolved and quantified basically as described earlier (24) and modified as follows: FAMEs were resolved using a Thermo Finnigan Trace GC 2000 system (Thermo Fisher Scientific Inc., Waltham, MA) equipped with an RTX-2330 capillary column (0.25 mm inner diameter × 30 m length; Restek, Bellefonte, PA). The inlet/injector was set to 220°C with a 10 ml/min split flow rate, a 1:10 split ratio, and a constant 1 ml/min carrier gas flow rate. A temperature program of 100°C for 1 min, 10°C/min to 140°C for 1 min, 2°C/min to 220°C for 1 min, and then ramp at 10°C/min to 260°C for 10 min was used to resolve individual FAMEs. Xcalibur version 1.3 software (Thermo Fisher Scientific Inc.) was used to detect, identify, and quantitate FAME peaks obtained with two different detection systems: *1*) for quantitation, a flame ionization detector in the Finnigan Trace GC2000 system; and *2*) for identification, chemical and electron ionization sources in a Trace DSQ version 1.3.1 mass spectrophotometer detector. Individual peaks were identified by comparison of retention times, as well as parental ion molecular weights and fragmentation pattern matching using the Xcalibur 1.3 ion fragmentation library with those of known methyl ester standards of even-number fatty acids, branched-chain FAMEs (phytanic methyl ester, pristanic methyl ester), and 15:0-ME internal standard, as described earlier (52). Identified FAME peaks were then referenced against the internal standard (15:0-ME) for quantification.

Calculations and statistics

Data for individual fatty acids were calculated both as nanomoles per milligram liver protein and as percent distribution. Fatty acids were also subgrouped according to total, total branched chain, total saturated, total unsaturated, total monounsaturated, and total polyunsaturated fatty acids expressed as nanomoles per milligram liver protein or as a percent of total liver fatty acids. The peroxidizability index was calculated as described (53). All values are expressed as mean ± SEM with "n" indicated. Statistical analysis was performed using one-way ANOVA analysis with Newman-Keuls paired comparisons posttest (GraphPad Prism, San Diego, CA). Values with $P \leqslant 0.05$ were considered statistically significant.

RESULTS

FABP1 and SCP-2 binding specificity for phytol and phytanic acid: ANS fluorescence displacement

It is not known whether FABP1 and/or SCP-2 impact hepatic phytol metabolism by directly binding phytol itself and/or by binding phytol metabolites (e.g., phytanic acid). The former possibility is suggested by FABP1 and SCP-2 binding certain other types of fatty alcohols. For example, FABP1 binds unsaturated branched-chain alcohol retinol (54, 55), alcohol eicosanol (55), and polycyclic branched-side chain alcohols, such as cholesterol (37) and estradiol (55). Likewise, SCP-2 binds cholesterol, a polycyclic alcohol with a branched-side chain (9, 56, 57). Therefore, it was important to determine whether FABP1 and/or SCP-2 directly bind phytol and/or just phytol metabolites, such as phytanic acid. The ability of FABP1 and SCP-2 to bind phytol was determined by displacement of bound ANS, a synthetic fluorophore, as described in the Materials and Methods.

Phytol did not significantly displace ANS from FABP1 or SCP-2, even at very high phytol concentration (33 μM) that was nearly 80-fold higher than the protein concentration (**Fig. 1A**). Tyrosine quenching and protein bound NBD-stearate displacement assays confirmed that FABP and SCP2 did not bind phytol or bound phytol with very weak affinity, at least several orders of magnitude higher than

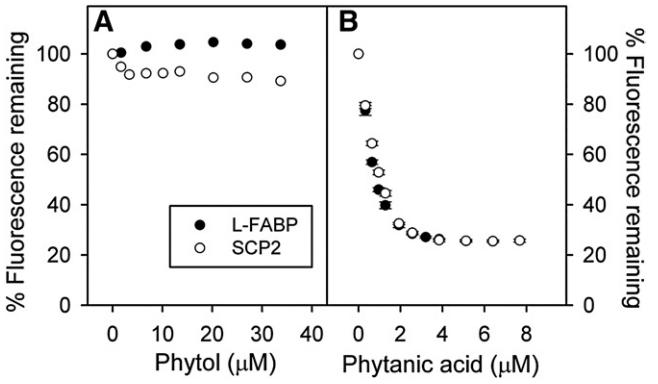

Fig. 1. Displacement of FABP1 and SCP-2 bound ANS by phytol versus phytanic acid. FABP1 (500 nM, closed circle) with ANS (35 μM) or SCP-2 (500 nM, open circle) with ANS (50 μM) were titrated with increasing amounts of phytol (A) or phytanic acid (B). ANS fluorescence remaining was measured by scanning 410–600 nm with excitation at 380 nm as described in the Materials and Methods. Values represent average percent remaining ANS fluorescence ± standard error (n = 4–5).

the K_i of phytanic acid (see below). In contrast, the phytol metabolite phytanic acid readily displaced FABP1 and SCP-2 bound ANS with essentially superimposable displacement curves (Fig. 1B). Based on the known affinity of each protein for ANS, as described in Materials and Methods, the K_i of phytanic acid for displacing ANS from FABP1 and SCP-2 was calculated to be 39 ± 3 nM and 125 ± 6 nM, respectively.

Because phytanic acid is produced from phytol in the endoplasmic reticulum, these findings suggested that cytosolic FABP1 and SCP-2 do not facilitate phytol metabolism by binding/transfer of diet-derived phytol to the liver endoplasmic reticulum for metabolism.

Impact of TKO and dietary phytol on hepatic branched-chain fatty acid accumulation

In vitro ligand binding (Fig. 1) and studies with transfected cells individually overexpressing FABP1, SCP-2, or SCP-x (23, 35) suggest that all three proteins facilitate hepatic phytol metabolism. However, interpreting the in vivo significance of loss of these proteins in *Scp-2/Scp-x*-null (17, 21, 36) or *Scp-x*-null mice (24) is complicated by concomitant upregulation of FABP1. To circumvent the concomitant upregulation of FABP1, *Fabp1* gene ablated mice were crossed with *Scp-2/Scp-x*-null mice to create *Fabp1/Scp-2/Scp-x*-null (i.e., TKO), mice as described in the Materials and Methods.

In control-fed mice, TKO differentially impacted hepatic accumulation of LCFAs. TKO had no effect on branched-chain fatty acids, which were not detectable in livers of control-diet-fed female or male WT mice (**Fig. 2A**, B). In contrast, TKO elicited a sex-dependent decrease in hepatic accumulation of fatty acids in female (Fig. 2C), but not male (Fig. 2D), mice. Thus, total LCFAs were significantly lower in female TKO mice (Fig. 2E) with no affect observed in the male TKO mice (Fig. 2F).

Phytol-diet induced hepatic accumulation of branched-chain LCFAs in both WT and TKO female mice with a

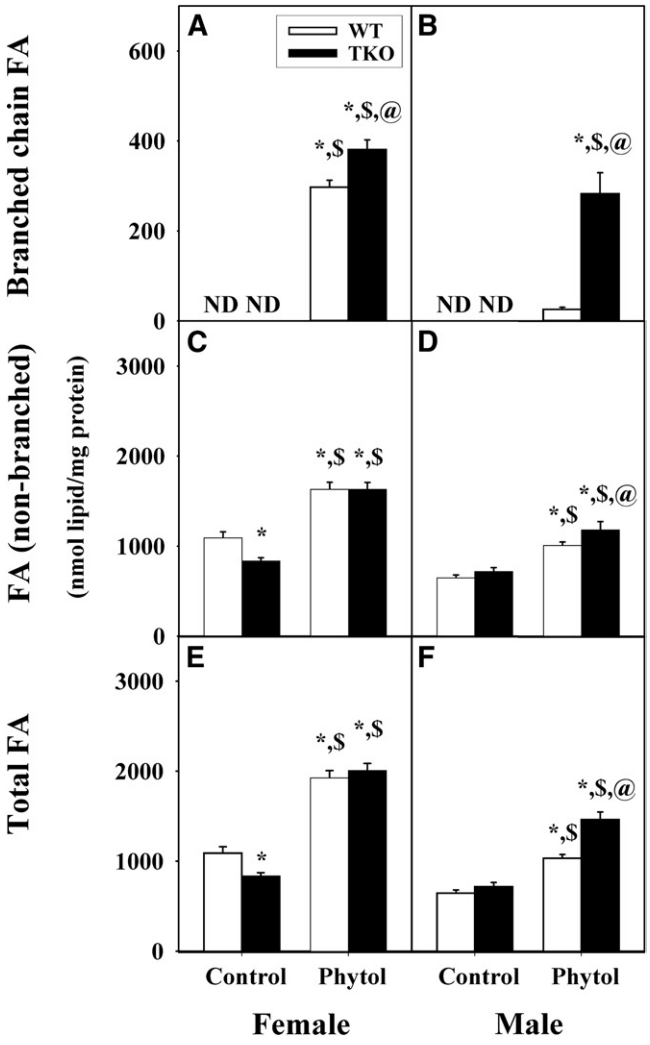

Fig. 2. Hepatic accumulation of branched-chain, nonbranched, and total fatty acids in WT and TKO mice fed dietary phytol. Female (A, C, E) and male (B, D, F) WT (open bars) and *Fabp1/Scp-2/Scp-x*-null (TKO) (black bars) mice were fed control or 0.5% phytol-supplemented chow as described in the Materials and Methods. Hepatic levels of branched-chain FA (A, B), FA (non-branched) (C, D), and total FA (E, F) were determined as described in the Materials and Methods. Values represent the mean nanomoles if fatty acid per milligrams total liver protein ± SE (n = 4–6); ND, not detected; $*P \leq 0.05$ versus WT on control-diet; $\$P \leq 0.05$ versus TKO on control-diet; $@P \leq 0.05$ versus WT on phytol-diet.

modest increase of the TKO over the WT (Fig. 2A). In the male TKO mice, there was a similar induction of hepatic accumulation of branched-chain LCFAs (Fig. 2A, B), but in the male WT mice, there was only a modest induction (Fig. 2B) such that the hepatic branched-chain content of the TKO males was 11-fold (Fig. 2B) more than the WT males. Phytol-diet also increased hepatic accumulation of LCFAs in both female and male mice (Fig. 2C, D). The latter effect was exacerbated by TKO in male, but not female, phytol-fed mice (Fig. 2C, D). Together these changes increased the hepatic level of total LCFAs by 1.8-fold in both female and male WT mice, with the effect being magnified in male TKO mice fed phytol-diet (Fig. 2E, F).

Thus, female WT mice appeared much more sensitive to dietary phytol than their male counterparts, as evidenced

by much higher hepatic accumulation of branched-chain LCFAs. TKO exacerbated hepatic accumulation of branched-chain LCFA in phytol-fed female mice and even more so phytol-fed male mice. In contrast, TKO decreased accumulation of LCFAs in female, but not male, mice fed control-diet, but increased that in phytol-fed male (but not female) mice.

TKO induces hepatic accumulation of phytol metabolite produced in endoplasmic reticulum (phytanic acid)

FABP1 is primarily localized in liver cytosol (58, 59). Overexpression of FABP1 in L-cell fibroblasts enhances (23, 25), while *Fabp1* gene ablation inhibits (26), branched-chain fatty acid oxidation. Thus, it was important to determine whether TKO selectively induced accumulation of the first phytol-metabolite (i.e., phytanic acid) produced from phytol in the endoplasmic reticulum.

Although phytanic acid was not detected in WT female or male mice fed control-diet (**Fig. 3A–**F), phytol-diet elicited sex-dependent accumulation of phytanic acid, the major hepatic metabolite of phytol in liver. Phytanic acid accumulation was nearly 8-fold greater in phytol-fed WT female than WT male mice (Fig. 3A, B). TKO modestly enhanced hepatic accumulation of phytanic acid in females (Fig. 3A) and markedly exacerbated phytanic acid accumulation in males (Fig. 3B). When phytanic acid was expressed as a percent of total fatty acid, TKO again increased phytanic acid accumulation in phytol-fed TKO females and, even more so, TKO males (supplemental Fig. S1). Only when phytanic acid was expressed as percent of liver total branched-chain LCFAs, did the percent phytanic acid not differ between phytol-fed male and female WT and TKO mice (**Fig. 4A**, B).

Taken together, these findings showed that the greater hepatic accumulation of phytanic acid in phytol-fed WT females than males correlated with the females' markedly lower expression of FABP1, SCP-2, and SCP-x than WT males (60, 61), perhaps analogous to partial "knock-down" of these proteins involved in phytol metabolism. This possibility was supported by the finding that complete ablation of all three proteins (i.e., TKO) resulted in a much greater quantitative loss of FABP1, SCP-2, and SCP-x in male than female mice and, thereby correspondingly, in greater increase in phytanic acid accumulation in phytol-fed TKO males than their female counterparts.

TKO induces hepatic accumulation of peroxisomal metabolites (pristanic acid and 2,3-pristenic acid) from phytanic acid

Once transported into the peroxisomal matrix, phytanic acid is further metabolized to pristanic acid and, subsequently, to 2,3-pristenic acid (62). Nearly half of SCP-2 and all of SCP-x are localized in peroxisomes (10, 11, 22–24, 63). Thus, it was important to determine whether TKO enhanced accumulation of peroxisomal metabolites of phytanic acid.

Although pristanic acid and 2,3-pristenic acid were not detected in WT or TKO mice fed control-diet (Fig. 3C–F), phytol-fed mice exhibited sex-dependent accumulation of phytol metabolites. Although present at lower levels than

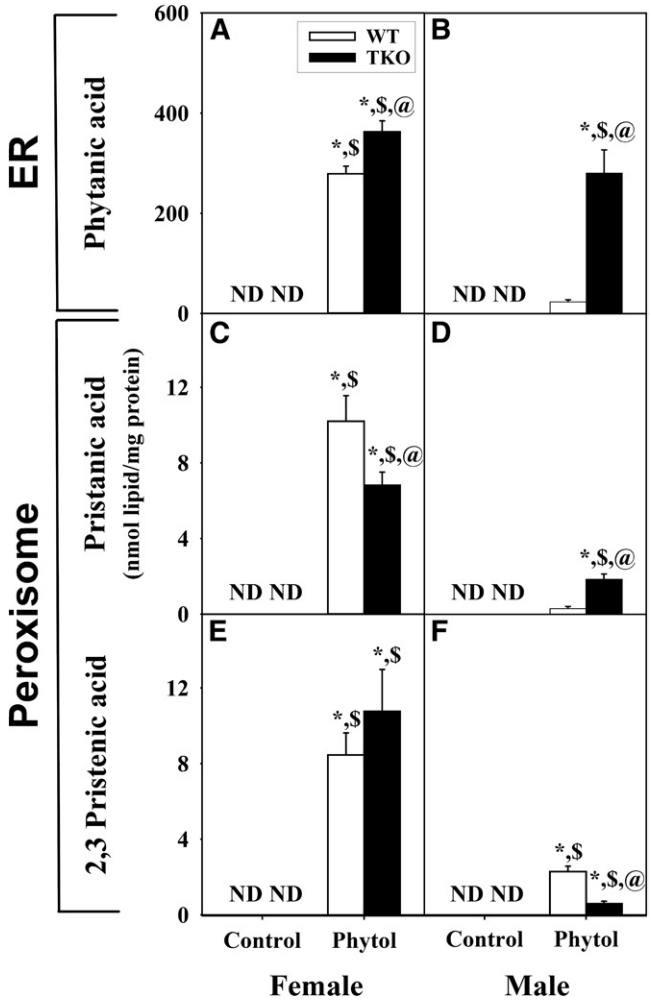

Fig. 3. Mass distribution of phytol metabolites in hepatic lipids of WT and TKO mice fed dietary phytol. Female (A, C, E) and male (B, D, F) WT (white bars) and *Fabp1/Scp-2/Scp-x*-null (TKO) (black bars) mice were fed control or 0.5% phytol-supplemented chow as described in the Materials and Methods. Liver lipids were extracted and analyzed by GC-MS to determine the contents (nanomoles per milligram protein) of phytanic acid (A, B), pristanic acid (C, D), and Δ2,3-pristenic acid (E, F) as described in the Materials and Methods. Values represent the mean nanomoles of fatty acie per milligram of total liver protein ± SE (n = 4–8); ND, not detected; $*P \leq 0.05$ versus WT control-diet; $\$P \leq 0.05$ versus TKO control-diet; $@P \leq 0.05$ versus WT phytol-diet.

phytanic acid in phytol-fed WT mice, these peroxisomal metabolites were detectable in phytol-fed female mice (Fig. 3C, E) and less so phytol-fed male mice (Fig. 3D, F). In phytol-fed mice, TKO decreased hepatic accumulation of pristanic acid in females (Fig. 3C), but increased the accumulation in males (Fig. 3D). Both phytol-fed WT and TKO female mice had significant accumulation of 2,3-pristenic acid without any differential impact by the TKO (Fig. 3E). However in phytol-fed male mice, the accumulation of 2,3-pristenic acid was much less than in the females (Fig. 3F). Furthermore the TKO exhibited significantly less accumulation of 2,3-pristenic acid than the WT (Fig. 3F). A similar pattern was observed when these metabolites were expressed as a percent of total fatty acids (supplemental Fig. S1). Only when expressed as percent of liver total

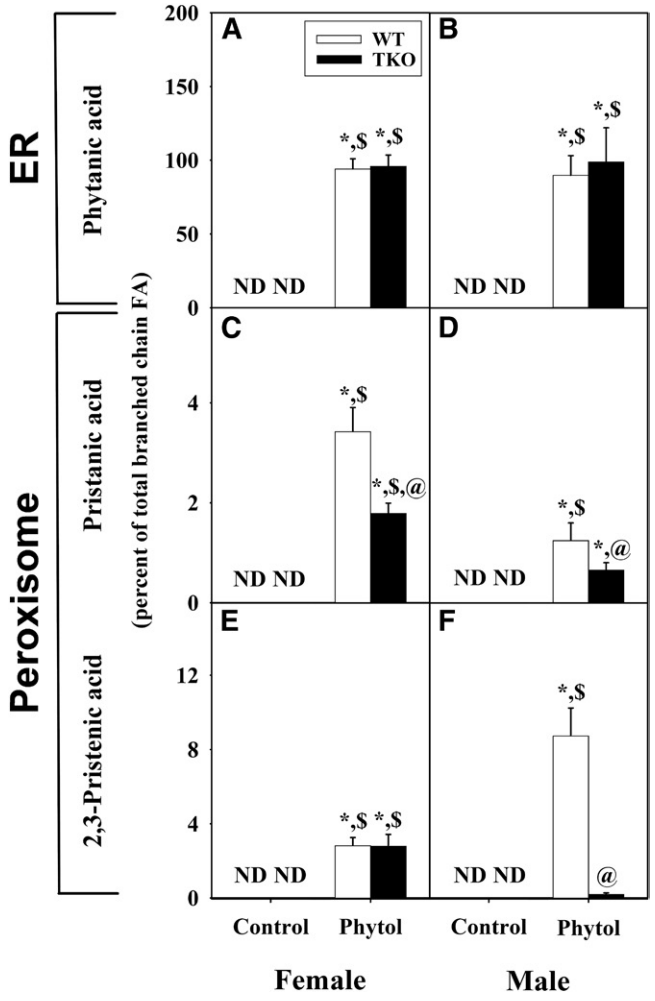

Fig. 4. Relative proportion of phytol metabolites as percent of total branched-chain fatty acid content. Liver lipids were extracted and analyzed by GC-MS to determine the relative proportions of phytanic acid (A, B), pristanic acid (C, D), and Δ2,3-pristenic acid (E, F) as described in the Material and Methods. Values represent the mean percent of total liver branched chain fatty acid ± SE (n = 4–6); ND, not detected; *$P \leq 0.05$ versus WT control-diet; $$P \leq 0.05$ versus TKO control-diet; @$P \leq 0.05$ versus WT phytol-diet.

branched-chain LCFAs, did TKO decrease the percent pristanic acid similarly in both males and females (Fig. 4C, D), while the percent 2,3-pristenic acid was decreased markedly in males, but not in females (Fig. 4E, F).

Thus, loss of L-FABP, SCP-2, and SCP-x in TKO mice differentially increased hepatic accumulation of phytanic acid metabolites produced in peroxisomes, increasing that of pristanic acid, but decreasing that of 2,3-pristenic acid, in phytol-fed males. Concomitantly, TKO decreased accumulation of pristanic acid, but not 2,3-pristenic acid in phytol-fed females. Taken together, these data suggested that loss SCP-2/SCP-x in TKO mice subtly impacted accumulation of peroxisomal metabolites of phytanic acid, but did not result in their massive accumulation.

Impact of TKO on hepatic accumulation of saturated and unsaturated fatty acids

Fabp1 and/or *Scp-2/Scp-x* gene product proteins enhance LCFA mitochondrial oxidation by: *1*) enhancing LCFA uptake/targeting of bound LCFA to mitochondria (64–68); *2*) directly binding to the cytosol facing LCFA-CoA binding domain of carnitine palmitoyl-1 acyltransferase (CPT1A), the rate limiting enzyme in mitochondrial LCFA oxidation, to stimulate LCFA-CoA utilization for oxidation (69); *3*) targeting nuclei to bind PPARα and facilitate ligand (LCFA, LCFA-CoA) activation of transcription of LCFA oxidative genes (70–72). Because phytol metabolites (phytanic acid, pristanic acid) are the most potent known natural activators of PPARα transcriptional activity (46), the possibility that TKO may also impact the hepatic proportion of saturated or unsaturated LCFAs was examined. The total mass content and percent composition of each class of LCFA (i.e., saturated, unsaturated, monounsaturated, polyunsaturated) was determined from the complete mass content (supplemental Tables S1, S3) and percent composition (supplemental Tables S2, S4) of all LCFAs detected by GC-MS for hepatic lipids from WT and TKO, female and male, control-fed and phytol-fed mice indicated.

Dietary phytol increased hepatic mass (nanomoles per milligram protein) of saturated fatty acids in both WT male and WT female mice (**Fig. 5A**, B) at the expense of all other classes of fatty acids in WT females (supplemental Fig. S2C, E, G), but not WT males (supplemental Fig. S2D, F, H). When calculated as percent of total liver LCFAs, phytol-diet likewise increased the proportion of saturated LCFAs in WT females (supplemental Fig. S2A) at the expense of mostly MUFA (supplemental Fig. S2C, E, G). In contrast, those in WT males were not affected (supplemental Fig. S2B, D, F, H).

TKO, alone, did not alter hepatic mass (nanomoles per milligram protein) of saturated LCFAs in control-diet-fed female or male mice (Fig. 5A, B), even when expressed as percent of total nonbranched fatty acids (supplemental Fig. S2A, B). TKO exacerbated the impact of phytol diet on mass (nanomoles per milligram protein) accumulation of saturated LCFA accumulation in male, but not female mice (Fig. 5A, B). This trend was observed even when calculated as percent of total liver LCFAs (supplemental Fig. S2B). The latter increase was at the expense of all other LCFA classes (supplemental Fig. S2D, F, H). In contrast, those in WT females were not affected (supplemental Fig. S2A, C, E, G).

In summary, TKO selectively impacted not only total levels of hepatic LCFAs, but also selectively increased the levels of saturated LCFAs in phytol-fed male mice.

TKO selectively alters the effect of dietary phytol on hepatic saturated and unsaturated fatty acid ratios and peroxidizability index

The ratios of LCFAs for saturated/unsaturated, polyunsaturated/monounsaturated, and peroxidizability index were determined as described in the Materials and Methods from the complete LCFA mass (nanomoles per milligram) compositions detected by GC-MS for hepatic lipids from WT and TKO, female and male, control-fed and phytol-fed mice (supplemental Tables S1, S3).

When the content of LCFA classes was expressed as ratios or peroxidizability indices, phytol-diet increased the

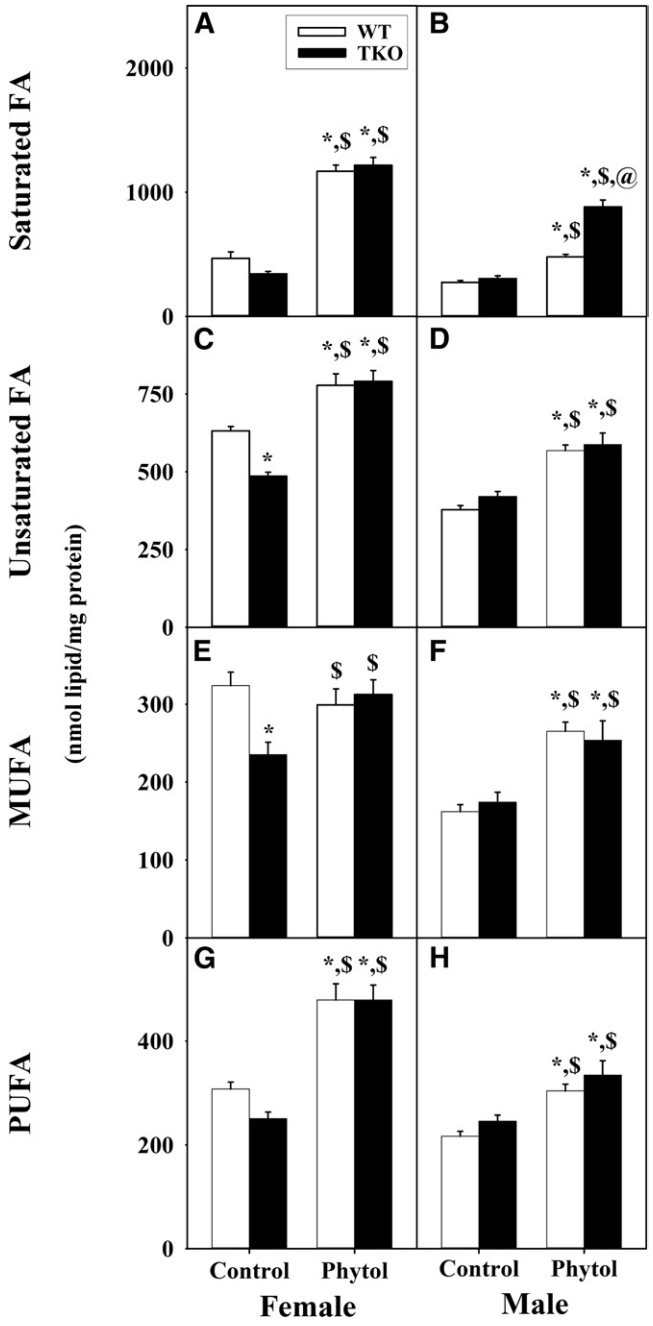

Fig. 5. Mass distribution of fatty acid subgroups in livers of WT and TKO mice fed dietary phytol. Female (A, C, E, G) and male (B, D, F, H) WT (white bars) and *Fabp1/Scp-2/Scp-x*-null (TKO) (black bars) mice were fed control or 0.5% phytol-supplemented chow as described. Liver lipids were extracted and quantities (nanomoles per milligram of protein) of total hepatic saturated (Sat) fatty acids (A, B), unsaturated (Unsat) fatty acids (C, D), MUFAs (E, F), and PUFAs (G, H) determined by GC-MS as described in the Materials and Methods. Values represent the mean nanomoles of fatty acid per milligram of total liver protein ± SE (n = 4–6); $*P \leq 0.05$ versus WT control-diet; $\$P \leq 0.05$ versus TKO control-diet; $@P \leq 0.05$ versus WT phytol-diet.

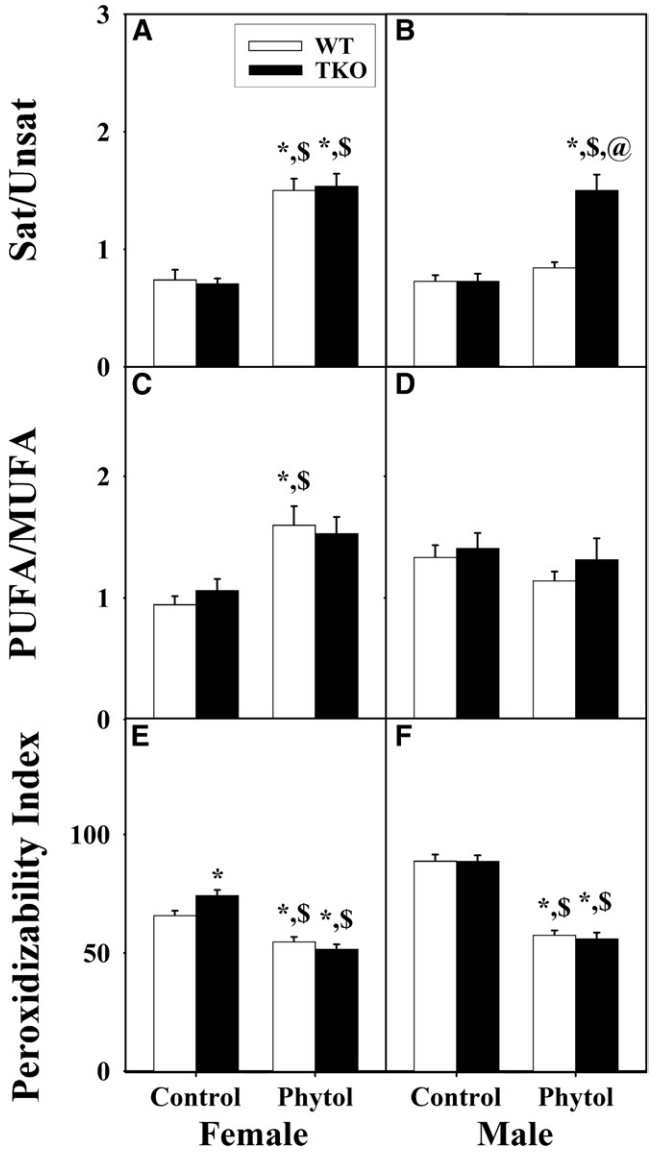

Fig. 6. Effect of TKO on hepatic fatty acid subgroup ratios and peroxidizability indices in phytol-fed mice. Female (A, C, E) and male (B, D, F) WT (white bars) and *Fabp1/Scp-2/Scp-x*-null (TKO) (black bars) mice were fed control or 0.5% phytol-supplemented chow. Ratios of saturated fatty acid to unsaturated fatty acid (Sat/Unsat) (A, B) and PUFAs/MUFAs (C, D) were calculated using the corresponding hepatic fatty acid subgroup values in this figure. Peroxidizability indices (E, F) were calculated as described in the Materials and Methods and presented in the same format. Values represent the mean ratio (or index) ± SE (n = 4–6); $*P \leq 0.05$ versus WT control-diet; $\$P \leq 0.05$ versus TKO control-diet; $@P \leq 0.05$ versus WT phytol-diet.

saturated/unsaturated, as well as polyunsaturated/monounsaturated, fatty acid ratios in WT female (**Fig. 6A**, C), but not WT male (Fig. 6B, D), mice. Concomitantly, phytol-diet decreased the peroxidizability indices of both WT female (Fig. 6E) and WT male (Fig. 6F) mice. TKO alone had little effect on these indices in either control-fed or phytol-fed females (Fig. 6A, C, E) or control-fed males (Fig. 6B, D, F), and only modestly affected that in phytol-fed males by increasing the saturated/unsaturated LCFA ratio. The peroxidizability index was not, or only slightly, altered by TKO in either control-fed or phytol-fed male or female mice (Fig. 6E, F).

Taken together these data suggested that TKO selectively decreased the proportion of unsaturated (both mono- and polyunsaturated) LCFAs.

DISCUSSION

In contrast to our understanding of the role of cytosolic chaperone lipid binding proteins in LCFA metabolism, much less is known about how the dietary branched-chain phytol molecule and its metabolites are solubilized, transported, and/or presented to metabolic enzymes within liver hepatocytes. The available evidence suggests that three intracellular lipid binding proteins may contribute to branched-chain fatty acid metabolism: *1*) FABP1 (23, 25–27); *2*) SCP-2; and *3*) SCP-x, with the latter both encoded by a single *Scp-2/Scp-x* gene through alternate transcription sites (8, 10, 22–24). In vitro assays of ligand binding, stimulation of enzyme activity, and subcellular localization, as well as transfected cell studies from our laboratory and other laboratories support potential roles for FABP1, SCP-2, and SCP-x in hepatic phytol metabolism. However, the in vivo functions of these proteins in hepatic phytol metabolism have proven to be more difficult to interpret because effects of ablating *Scp-2/Scp*-x (17, 21, 36) or the alternate transcription site in *Scp-2/Scp*-x gene that controls transcription of SCP-x mRNA (24) may be counteracted, in part, by several-fold concomitant upregulation of FABP1.

To begin to address this issue, the physiological impact of a 0.5% phytol-diet on whole body and hepatic phenotype has been examined in both WT mice and in mice ablated for all three proteins, i.e., *Fabp1/Scp-2/Scp-x* null (TKO). In WT mice, both whole body and hepatic lipid phenotype correlated with WT females' significantly lower expression of FABP1, SCP-2, and SCP-x than WT males (60, 61). For example, despite similar food consumption, control-fed WT females had greater body weight gain and accumulated 3.4-fold more hepatic triacylglyceride than WT males (52). Further, phytol-diet alone did not alter food consumption in either male or female WT mice, but selectively reduced body weight in WT females, but not WT males (52). Finally, phytol-diet alone greatly reduced hepatic triacylglyceride accumulation by 77% in WT males, and less so, by 52% in WT females (52). Because nonalcoholic fatty liver disease (NAFLD) is characterized by hepatic lipid accumulation, these studies suggested that the lower hepatic expression of FABP1, SCP-2, and SCP-x in WT females may make females more susceptible to NAFLD, correlating with high-fat-induced NAFLD in some strains of female (73), but not male, mice (74), as well as with the higher prevalence of NAFLD in women (74, 75). Furthermore, phytol-diet made WT mice less susceptible to hepatic triacylglyceride accumulation, more so males than females and correlated with WT females having lower hepatic expression of FABP1, SCP-2, and SCP-x than WT males (60, 61).

Phenotypic effects of TKO in phytol-fed mice were sexual-dimorphic, more severe in males, and correlated with the WT male's higher basal expression of FABP1, SCP-2, and SCP-x than their female counterparts (60, 61). TKO elicited whole-body weight loss in phytol-fed, but not control-fed, male and female mice (60, 61). The TKO-induced weight loss in phytol-fed mice was: *i*) manifested proportionally in both lean tissue mass and fat tissue mass; *ii*) not associated with decreased food preference for phytol-diet; and *iii*) attributed primarily to markedly decreased food conversion efficiency in TKO males and less so in TKO females. Although phytol-diet induced mild hepatocellular necrosis and slightly elevated serum aspartate aminotransferase (AST) and alanine aminotransferase (ALT) in all male (data not shown) and female (60) groups, serum AST and ALT levels were all within the normal range. Nevertheless, concomitant with inducing whole body weight loss, TKO decreased liver weight in phytol-fed males (but not females), as well as increased hepatic lipid accumulation, especially phospholipid (more so in males than females.) The TKO-induced increase in phospholipid mass in phytol-fed mice was not compensated by a decrease in hepatic triacylglycerol (both males and females) or free cholesterol (males). The finding that serum levels of β-hydroxybutyrate (a physiological marker of fatty acid β-oxidation) were not significantly altered in either male or female phytol-fed TKO mice suggested that the above changes in whole-body and hepatic lipid phenotype were not associated with impaired fatty acid β-oxidation. Taken together, these findings indicated that TKO markedly exacerbated the impact of dietary phytol on the whole-body and liver phenotype of male and, less so, female mice. Thus, it was important to determine the extent (if any) to which the TKO-induced phenotype alterations in phytol-fed mice might be attributed to impaired metabolism of phytol. The data presented herein with phytol-fed male and female *Fabp1/Scp-2/Scp*-x-null (TKO) mice provide the following new insights:

First, FABP1 and SCP-2 bound phytol very poorly or not at all. This was unexpected because FABP1 is known to bind other branched-chain alcohols, such as retinol (54, 55), and alcohols, such as eicosanol (55). Furthermore, both SCP-2 and FABP1 bound polycyclic alcohols with branched-side chains (9, 37, 55–57). Thus, contrary to expectations, neither FABP1 nor SCP-2 appear as likely candidate chaperone proteins for transporting phytol from the plasma membrane to intracellular metabolic sites, i.e., endoplasmic reticulum and peroxisomes. Whether cellular retinol binding protein or an as yet unknown branched-chain lipid binding protein potentially serve as cytosolic phytol binding/chaperone protein remains to be resolved.

Second, loss of all three proteins in TKO mice (*Fabp1/Scp-2/Scp-x*-null) markedly enhanced accumulation of phytanic acid, the major phytol metabolite formed in the endoplasmic reticulum. Under phytol feeding, *Fabp1*-null mice also induced hepatic phytanic acid accumulation to a high extent (27), while *Scp-x* null mice elicited up to 8-fold less hepatic phytanic acid accumulation (24). However, concomitant upregulation of FABP1 in *Scp-x*-null mice may have compensated, in part, for the loss of SCP-x (24). Although the hepatic mass accumulation of phytanic acid was not reported in phytol-fed *Scp-2/Scp-x*-null mice, nearly 5-fold concomitant upregulation of FABP1 similarly complicates resolution of SCP-2/SCP-x contributions to hepatic phytol metabolism to phytanic acid (21). In contrast, as shown herein, ablation of all three proteins (TKO) elicited the highest hepatic accumulation of phytanic acid, the major metabolite of phytol. This may be explained by the fact that phytanic acid, produced in

the endoplasmic reticulum, must be transported to peroxisomes for further oxidation (5). FABP1 and/or SCP-2 are candidate proteins potentially serving this function because: *i*) both FABP1 and SCP-2 have high affinity for phytanic acid and phytanoyl-CoA, as shown herein (Fig. 1) and/or earlier with other types of binding assays for FABP1 (20, 33, 76, 77) and SCP-2 (20, 21, 78); *ii*) both FABP1 and SCP-2 enhance the cytosolic transport/diffusion of fatty acids (26, 65–67, 79); and *iii*) overexpression of SCP-2, SCP-x, or FABP1 enhanced (23, 25, 35), while *Fabp1* gene ablation inhibited, metabolism of [^{3}H]phytanic acid (26). However, FABP1 is nearly 8-fold more prevalent than SCP-2 in liver (17, 60, 69, 80, 81), and FABP1 is more highly distributed in cytosol than SCP-2 (half of SCP-2 is peroxisomal) (9–11). Taken together, these data would suggest FABP1 and, less so, SCP-2 as the major candidate chaperone proteins for transporting bound phytanic acid from the endoplasmic reticulum to peroxisome for further oxidation.

Third, the loss of all three proteins in TKO mice (*Fabp1/Scp-2/Scp-x* null) had a greater impact on hepatic phytanic acid accumulation in male than female phytol-fed mice. Livers of female WT mice normally have lower levels of FABP1, SCP-2, and/or SCP-x than their male counterparts (24, 52, 80). Consistent with these findings, livers of phytol-fed WT female mice also have higher phytanic acid than their male counterparts, as shown in (Fig. 3), and earlier (52). This suggested that the higher levels of these proteins in male mice would make their hepatic phytol metabolism more sensitive to complete loss of these proteins (e.g., TKO).

Fourth, TKO differentially altered the pattern of hepatic branched-chain phytol peroxisomal metabolites downstream from phytanic acid in phytol-fed female versus male mice. Several peroxisomal metabolites of phytanic acid (e.g., pristanic acid, 2,3-pristenic acid) were detected in the livers of male and female phytol-fed mice, but generally, at several orders of magnitude, lower levels than that of phytanic acid produced in the endoplasmic reticulum. This suggested that once phytanic acid is transported into the peroxisomes, it is very rapidly further metabolized. Nevertheless, TKO still significantly induced hepatic accumulation of pristanic acid, while concomitantly decreasing accumulation of the further downstream metabolite, 2,3-pristenic acid, in phytol-fed male mice. In contrast, levels of pristanic acid and 2,3-pristenic acid differed little between TKO and WT phytol-fed females, consistent with the already lower expression of SCP-2 and/or SCP-x in WT females, as compared with WT male mice (24, 52, 80). These findings were also consistent with the known subcellular distribution of SCP-2 and SCP-x, but not FABP1, in peroxisomes. SCP-2 is most highly concentrated in peroxisomes and SCP-x is exclusively localized in peroxisomes (9–11). In vitro ligand binding studies suggest that SCP-2 binds phytanoyl-CoA with high affinity, as well as less strongly binds several downstream metabolites (pristanic acid, phytenic acid, pristanoyl-CoA) within the peroxisomal matrix (20, 21). Although not itself exhibiting any enzyme activity, SCP-2 stimulates phytanoyl-CoA hydroxylation by phytanoyl-CoA hydroxylase, the enzyme mediating the first step in peroxisomal α-oxidation of branched-chain fatty acids (8). Furthermore, SCP-x is the only known branched-chain 3-ketoacyl-CoA thiolase that catalyzes cleavage of propionyl-CoA from 3-ketopristanoyl-CoA, a downstream peroxisomal metabolite of pristenoyl-CoA (82). Finally, when fed 0.5% phytol-diet, the TKO mice accumulated several fold higher levels of phytanic acid and pristanic acid (Fig. 3) than *Scp-x*-null mice on the same diet (24). A complicating factor, however, is that the phytol metabolite patterns in mice singly ablated for *Fabp1*, *Scp-x*, or *Scp-2/Scp-x* is complicated by compensatory changes in the nonablated proteins. For example, upregulation of SCP-x in *Fabp1* gene ablated mice yielded a phytol-metabolism pattern consistent with increased peroxisomal metabolites in phytol-fed male, but not female, mice (27). Likewise, altered FABP1 expression in response to singly ablating *Scp-x* resulted in a phytol metabolite pattern consistent with decreased extraperoxisomal (females) and peroxisomal (males) phytol metabolism (24). Conversely, massive upregulation of FABP1 in *Scp-2/Scp-x*-null mice resulted in a phytol metabolite pattern consistent with both increased accumulation of extraperoxisomal metabolite (phytanic acid), as well as altered pattern of peroxisomal metabolites (21). Taken together, these findings suggest that TKO not only elicited hepatic accumulation of phytanic acid (phytol metabolite produced in endoplasmic reticulum), it also more subtly altered the pattern of peroxisomal metabolites of phytanic acid further downstream.

Fifth, TKO differentially impacted hepatic levels of total LCFAs. While phytol-diet increased total LCFAs in both male and female WT mice, TKO had little further effect on exacerbating this accumulation. Furthermore, with regard to the hepatic content of total 22:6n-3, in the female mice there was a profound reduction in 22:6n-3 that was not found in the male mice. More importantly, the male values for 22:6n-3 in the WT and TKO were similar to the level found in the TKO female mouse. The phytol diet enhanced the amount in WT versus TKO mice (female) and the opposite was seen in the male mice. This suggested a significant difference that is sex-based on 22:6n-3 metabolism. As the Sprecher pathways involve the peroxisome, this was consistent with important roles for FABP1, SCP-2, and SCP-x in peroxisomal fatty acid metabolism as outlined in the Introduction. With regard to the sex-specificity, this may be attributed to at least two factors: *i*) Control-fed WT females having less hepatic FABP1, SCP-2, and SCP-x than WT males (60, 61). FABP1 overexpression stimulates (23), while *Fabp1* gene ablation inhibits, phytanic and pristanic acid metabolism (26, 27). Similarly, SCP-2 or SCP-x overexpression enhances (25, 35), while *Scp-x* (24) or *Scp-2/Scp-x* (22, 83, 84) ablation inhibits metabolism of branched-chain fatty acids. Thus, as shown herein, the phytol-fed TKO males and females accumulated 6-fold and 20% more phytol metabolites (especially phytanic acid and pristanic acid), the most potent known ligand activators of PPARα, nuclear receptor that controls expression of many genes in fatty acid metabolism, especially in peroxisomes (33, 45, 47); *ii*) Estrogens inhibit the actions

of PPARα agonists (85). Finally, it is important to note that the finding of phytol-induced hepatic total LCFA accumulation was in marked contrast to earlier studies wherein the respective proteins were singly ablated. For example, compensatory alterations in SCP-x expression in phytol-fed singly ablated *Fabp1*-null mice resulted in unaltered hepatic total LCFAs (27). Likewise, compensatory alterations in FABP1 expression in phytol-fed *Scp-x*-null mice resulted in unaltered levels of hepatic total LCFAs (24). Upregulation of FABP1 in *Scp-2/Scp-x*-null mice also complicated determination of these proteins' impact on hepatic total LCFA levels (21).

Taken together, the finding that neither FABP1 nor SCP-2 bound phytol suggested that neither protein likely contributed to directly enhance hepatic uptake of phytol (**Fig. 7**). Ablation of the *Fabp1*, as well as the *Scp-2/Scp-x* gene, created TKO mice, thereby precluding the known marked (5-fold) compensatory upregulation of FABP1 in *Scp-2/Scp-x*-null mice (21). The phytanic acid binding affinities and hepatic pattern of branched-chain LCFAs in phytol-fed TKO mice suggested that FABP1 is more involved than SCP-2 in binding/transfer of phytanic acid (produced in the endoplasmic reticulum) through the cytosol to peroxisomes, wherein SCP-2 and SCP-x function in binding/transport of phytanoyl-CoA for further metabolism by peroxisomal enzymes (Fig. 7). These findings complemented and helped to clarify earlier studies with phytol-fed mice wherein singly ablating the respective proteins elicited concomitant upregulation of nonablated protein (21, 24, 27).

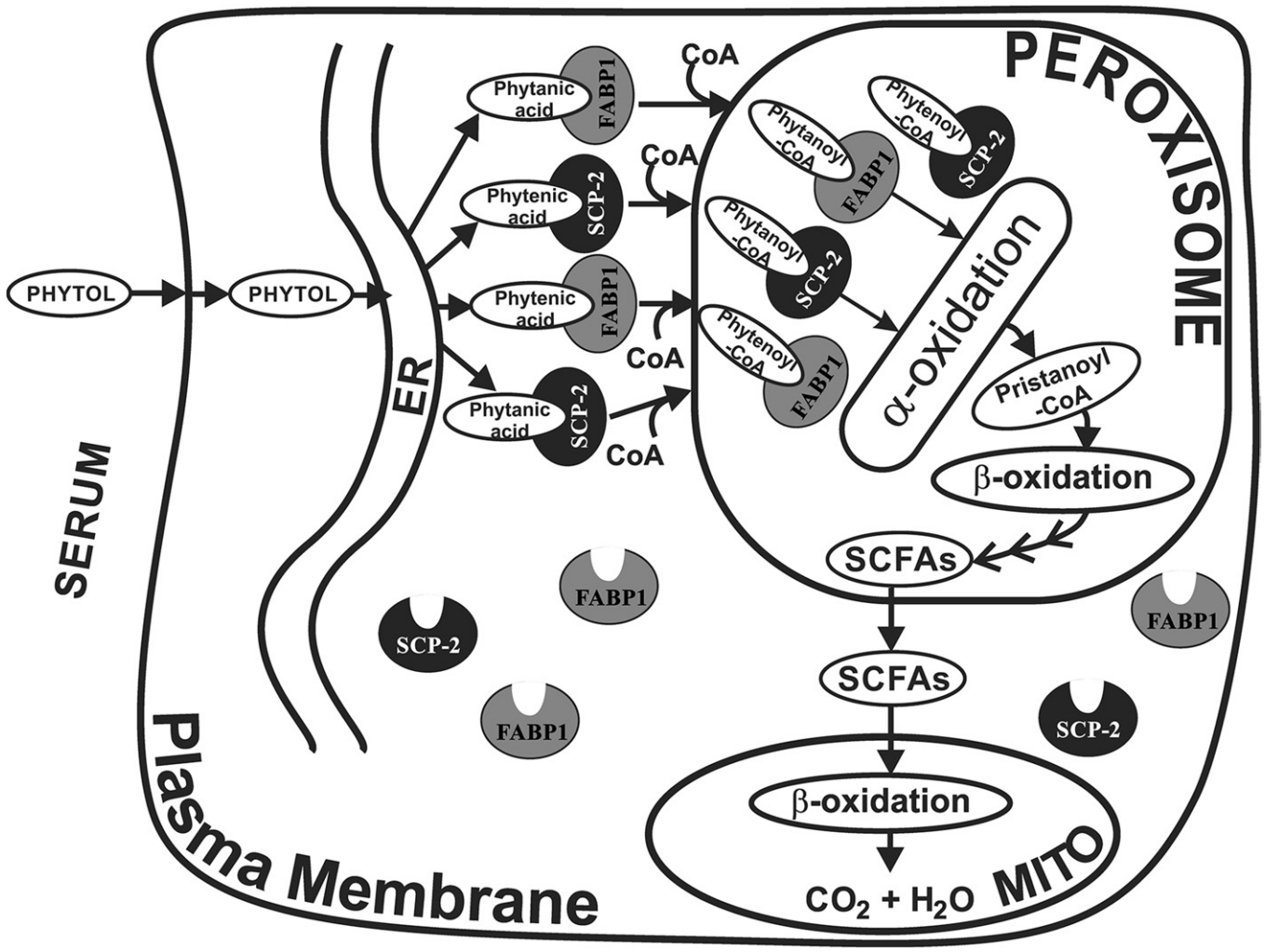

Fig. 7. Schematic of proposed FABP1 and SCP-2/SCP-x interactions with the phytol metabolic pathway. FABP1 and SCP-2, both present at high level in hepatic cytoplasm, bind phytol metabolites, but not phytol. In this hypothetical scheme, FABP1 and SCP-2 bind phytanic acid and phytenic acid (formed from phytol in the endoplasmic reticulum) and transport them to the peroxisome. At the peroxisomal membrane the phytanic and phytenic acid are converted to their respective CoA thioesters, internalized and desorbed into the peroxisomal matrix wherein they are bound (20, 21) by peroxisomal localized SCP-2 (9–11) and potentially FABP1 (34). Within the peroxisomal matrix, SCP-2 directly interacts with oxidative enzymes and stimulates phytanoyl-CoA 2-hydroxylase, the essential enzyme mediating the first step in peroxisomal α-oxidation of branched-chain fatty acids (8, 19). SCP-x, an exclusively peroxisomal protein, is the only known branched-chain 3-ketoacyl CoA thiolase (10, 22–24). Successive cycles of α- and β-oxidation shortens the branched-chain fatty acids to yield short-chain (<C12) fatty acids (SCFAs), such as formyl-CoA, acetyl-CoA, propionyl-CoA, and 4,8-dimethyl nonanoyl-CoA. Neither FABP1 (38, 86–88) nor SCP-2 (20, 40) binds short-chain (<C12) fatty acids or their CoA thioesters.

REFERENCES

1. Verhoeven, N. M., and C. Jakobs. 2001. Human metabolism of phytanic acid and pristanic acid. *Prog. Lipid Res.* **40:** 453–466.
2. Jansen, G. A., and R. J. A. Wanders. 2006. Alpha oxidation. *Biochim. Biophys. Acta.* **1763:** 1403–1412.
3. Steinberg, D. 1978. Phytanic acid storage disease: Refsum's syndrome. *In* The Metabolic Basis of Inherited Disease. J. B. Stanbury, J. B. Wyngaarden, and D. S. Fredrickson, editors. McGraw-Hill, New York. 688–706.
4. Steinberg, D. 1995. Refsums disease. *In* The Metabolic and Molecular Basis of Inherited Disease. C. R. Scriver, A. L. Beaudet, W. S. Sly, et al., editors. McGraw-Hill, New York. 2351–2370.
5. Gloerich, J., D. M. van der Brink, J. P. N. Ruiter, N. van Vlies, F. M. Vaz, R. J. A. Wanders, and S. Ferdinandusse. 2007. Metabolism of phytol to phytanic acid in the mouse, and the role of PPARalpha in its regulation. *J. Lipid Res.* **48:** 77–85.
6. Wanders, R. J. A., and H. R. Waterham. 2006. Biochemistry of mammalian peroxisomes revisited. *Annu. Rev. Biochem.* **75:** 295–332.
7. Wanders, R. J. A., P. Vreken, S. Ferdinandusse, G. A. Jansen, H. R. Waterham, C. W. van Roermund, and E. G. van Grunsven. 2001. Peroxisomal fatty acid alpha and beta oxidation in humans: enzymology, peroxisomal metabolite transporters and peroxisomal diseases. *Biochem. Soc. Trans.* **29:** 250–267.
8. Mukherji, M., N. J. Kershaw, C. J. Schofield, A. S. Wierzbicki, and M. D. Lloyd. 2002. Utilization of sterol carrier protein-2 by phytanoyl-CoA 2-hydroxylase in the peroxisomal alpha oxidation of phytanic acid. *Chem. Biol.* **9:** 597–605.
9. Martin, G. G., H. A. Hostetler, A. L. McIntosh, S. E. Tichy, B. J. Williams, D. H. Russell, J. M. Berg, T. A. Spencer, J. A. Ball, A. B. Kier, et al. 2008. Structure and function of the sterol carrier protein-2 (SCP-2) N-terminal pre-sequence. *Biochemistry.* **47:** 5915–5934.
10. Gallegos, A. M., B. P. Atshaves, S. M. Storey, O. Starodub, A. D. Petrescu, H. Huang, A. McIntosh, G. Martin, H. Chao, A. B. Kier, et al. 2001. Gene structure, intracellular localization, and functional roles of sterol carrier protein-2. *Prog. Lipid Res.* **40:** 498–563.
11. Keller, G. A., T. J. Scallen, D. Clarke, P. A. Maher, S. K. Krisans, and S. J. Singer. 1989. Subcellular localization of sterol carrier protein-2 in rat hepatocytes: its primary localization to peroxisomes. *J. Cell Biol.* **108:** 1353–1361.
12. Parr, R. D., G. G. Martin, H. A. Hostetler, M. E. Schroeder, K. D. Mir, A. B. Kier, J. M. Ball, and F. Schroeder. 2007. A new N-terminal recognition domain in caveolin-1 interacts with sterol carrier protein-2 (SCP-2). *Biochemistry.* **46:** 8301–8314.
13. Schroeder, F., B. P. Atshaves, A. L. McIntosh, A. M. Gallegos, S. M. Storey, R. D. Parr, J. R. Jefferson, J. M. Ball, and A. B. Kier. 2007. Sterol carrier protein-2: new roles in regulating lipid rafts and signaling. *Biochim. Biophys. Acta.* **1771:** 700–718.
14. Zhou, M., R. D. Parr, A. D. Petrescu, H. R. Payne, B. P. Atshaves, A. B. Kier, J. A. Ball, and F. Schroeder. 2004. Sterol carrier protein-2 directly interacts with caveolin-1 in vitro and in vivo. *Biochemistry.* **43:** 7288–7306.
15. Atshaves, B. P., A. Gallegos, A. L. McIntosh, A. B. Kier, and F. Schroeder. 2003. Sterol carrier protein-2 selectively alters lipid composition and cholesterol dynamics of caveolae/lipid raft vs non-raft domains in L-cell fibroblast plasma membranes. *Biochemistry.* **42:** 14583–14598.
16. Atshaves, B. P., J. R. Jefferson, A. L. McIntosh, B. M. McCann, K. Landrock, A. B. Kier, and F. Schroeder. 2007. Effect of sterol carrier protein-2 expression on sphingolipid distribution in plasma membrane lipid rafts/caveolae. *Lipids.* **42:** 871–884.
17. Atshaves, B. P., A. L. McIntosh, H. R. Payne, A. M. Gallegos, K. Landrock, N. Maeda, A. B. Kier, and F. Schroeder. 2007. Sterol carrier protein-2/sterol carrier protein-x gene ablation alters lipid raft domains in primary cultured mouse hepatocytes. *J. Lipid Res.* **48:** 2193–2211.
18. Matveev, S., A. Uittenbogaard, D. van Der Westhuyzen, and E. J. Smart. 2001. Caveolin-1 negatively regulates SRB1 mediated selective uptake of high density lipoprotein-derived cholesteryl ester. *Eur. J. Biochem.* **268:** 5609–5616.
19. Wouters, F. S., P. I. Bastiaens, K. W. Wirtz, and T. M. Jovin. 1998. FRET microscopy demonstrates molecular association of non-specific lipid transfer protein (nsL-TP) with fatty acid oxidation enzymes. *EMBO J.* **17:** 7179–7189.
20. Frolov, A., K. Miller, J. T. Billheimer, T-C. Cho, and F. Schroeder. 1997. Lipid specificity and location of the sterol carrier protein-2 fatty acid binding site: a fluorescence displacement and energy transfer study. *Lipids.* **32:** 1201–1209.
21. Seedorf, U., M. Raabe, P. Ellinghaus, F. Kannenberg, M. Fobker, T. Engel, S. Denis, F. Wouters, K. W. A. Wirtz, R. J. A. Wanders, et al. 1998. Defective peroxisomal catabolism of branched fatty acyl coenzyme A in mice lacking the sterol carrier protein-2/sterol carrier protein-x gene function. *Genes Dev.* **12:** 1189–1201.
22. Seedorf, U., P. Ellinghaus, and J. R. Nofer. 2000. Sterol carrier protein-2. *Biochim. Biophys. Acta.* **1486:** 45–54.
23. Atshaves, B. P., S. Storey, H. Huang, and F. Schroeder. 2004. Liver fatty acid binding protein expression enhances branched-chain fatty acid metabolism. *Mol. Cell. Biochem.* **259:** 115–129.
24. Atshaves, B. P., A. L. McIntosh, D. Landrock, H. R. Payne, J. Mackie, N. Maeda, J. M. Ball, F. Schroeder, and A. B. Kier. 2007. Effect of SCP-x gene ablation on branched-chain fatty acid metabolism. *Am. J. Physiol. Gastrointest. Liver Physiol.* **292:** G939–G951.
25. Atshaves, B. P., S. M. Storey, A. D. Petrescu, C. C. Greenberg, O. I. Lyuksyutova, R. Smith, and F. Schroeder. 2002. Expression of fatty acid binding proteins inhibits lipid accumulation and alters toxicity in L-cell fibroblasts. *Am. J. Physiol. Cell Physiol.* **283:** C688–C703.
26. Atshaves, B. P., A. L. McIntosh, O. I. Lyuksyutova, W. R. Zipfel, W. W. Webb, and F. Schroeder. 2004. Liver fatty acid binding protein gene ablation inhibits branched-chain fatty acid metabolism in cultured primary hepatocytes. *J. Biol. Chem.* **279:** 30954–30965.
27. Atshaves, B. P., A. L. McIntosh, H. R. Payne, J. Mackie, A. B. Kier, and F. Schroeder. 2005. Effect of branched-chain fatty acid on lipid dynamics in mice lacking liver fatty acid binding protein gene. *Am. J. Physiol. Cell Physiol.* **288:** C543–C558.
28. McIntosh, A. L., B. P. Atshaves, S. M. Storey, K. K. Landrock, D. Landrock, G. G. Martin, A. B. Kier, and F. Schroeder. 2012. Loss of liver fatty acid binding protein impacts mouse hepatocyte plasma membrane microdomains. *J. Lipid Res.* **53:** 467–480.
29. Huang, H., A. L. McIntosh, G. G. Martin, K. Landrock, D. Landrock, S. Gupta, B. P. Atshaves, A. B. Kier, and F. Schroeder. 2014. Structural and functional interaction of fatty acids with human liver fatty acid binding protein (L-FABP) T94A variant. *FEBS J.* **281:** 2266–2283.
30. Martin, G. G., A. L. McIntosh, H. Huang, S. Gupta, B. P. Atshaves, A. B. Kier, and F. Schroeder. 2013. Human liver fatty acid binding protein (L-FABP) T94A variant alters structure, stability, and interaction with fibrates. *Biochemistry.* **52:** 9347–9357.
31. Storey, S. M., A. L. McIntosh, H. Huang, G. G. Martin, K. K. Landrock, D. Landrock, H. R. Payne, A. B. Kier, and F. Schroeder. 2012. Loss of intracellular lipid binding proteins differentially impacts saturated fatty acid uptake and nuclear targeting in mouse hepatocytes. *Am. J. Physiol. Gastrointest. Liver Physiol.* **303:** G837–G850.
32. Wolfrum, C. 2007. Cytoplasmic fatty acid binding protein sensing fatty acids for peroxisome proliferator activated receptor activation. *Cell. Mol. Life Sci.* **64:** 2465–2476.
33. Wolfrum, C., P. Ellinghaus, M. Fobker, U. Seedorf, G. Assmann, T. Borchers, and F. Spener. 1999. Phytanic acid is ligand and transcriptional activator of murine liver fatty acid binding protein. *J. Lipid Res.* **40:** 708–714.
34. Antonenkov, V. D., R. T. Sormunen, S. Ohlmeier, L. Amery, and M. Fransen. 2006. Localization of a portion of the liver isoform of fatty acid binding protein (L-FABP) to peroxisomes. *Biochem. J.* **394:** 475–484.
35. Atshaves, B. P., S. M. Storey, and F. Schroeder. 2003. Sterol carrier protein-2/sterol carrier protein-x expression differentially alters fatty acid metabolism in L-cell fibroblasts. *J. Lipid Res.* **44:** 1751–1762.
36. Fuchs, M., A. Hafer, C. Muench, F. Kannenberg, S. Teichmann, J. Scheibner, E. F. Stange, and U. Seedorf. 2001. Disruption of the sterol carrier protein 2 gene in mice impairs biliary lipid and hepatic cholesterol metabolism. *J. Biol. Chem.* **276:** 48058–48065.
37. Martin, G. G., B. P. Atshaves, H. Huang, A. L. McIntosh, B. W. Williams, P-J. Pai, D. H. Russell, A. B. Kier, and F. Schroeder. 2009. Hepatic phenotype of liver fatty acid binding protein (L-FABP) gene ablated mice. *Am. J. Physiol. Gastrointest. Liver Physiol.* **297:** G1053–G1065.
38. Frolov, A., T. H. Cho, E. J. Murphy, and F. Schroeder. 1997. Isoforms of rat liver fatty acid binding protein differ in structure and affinity for fatty acids and fatty acyl CoAs. *Biochemistry.* **36:** 6545–6555.
39. Matsuura, J. E., H. J. George, N. Ramachandran, J. G. Alvarez, J. F. I. Strauss, and J. T. Billheimer. 1993. Expression of the mature and the pro-form of human sterol carrier protein 2 in Escherichia coli alters bacterial lipids. *Biochemistry.* **32:** 567–572.

40. Frolov, A., T. H. Cho, J. T. Billheimer, and F. Schroeder. 1996. Sterol carrier protein-2, a new fatty acyl coenzyme A-binding protein. *J. Biol. Chem.* **271:** 31878–31884.
41. Velkov, T. 2013. Interactions between human liver fatty acid binding protein and peroxisome proliferator activated receptor drugs. *PPAR Res.* **2013:** 938401.
42. Storey, S. M., B. P. Atshaves, A. L. McIntosh, K. K. Landrock, G. G. Martin, H. Huang, J. D. Johnson, R. D. Macfarlane, A. B. Kier, and F. Schroeder. 2010. Effect of sterol carrier protein-2 gene ablation on HDL-mediated cholesterol efflux from primary cultured mouse hepatocytes. *Am. J. Physiol. Gastrointest. Liver Physiol.* **299:** G244–G254.
43. Thigpen, J. E., K. D. Setchell, K. B. Ahlmark, J. Kocklear, T. Spahr, G. F. Caviness, M. F. Goelz, J. K. Haseman, R. R. Newbold, and D. B. Forsythe. 1999. Phytoestrogen content of purified, open- and closed-formula laboratory animal diets. *Lab. Anim. Sci.* **49:** 530–536.
44. Thigpen, J. E., K. D. Setchell, M. F. Goelz, and D. B. Forsythe. 1999. The phytoestrogen content of rodent diets. *Environ. Health Perspect.* **107:** A182–A183.
45. Ellinghaus, P., C. Wolfrum, G. Assmann, F. Spener, and U. Seedorf. 1999. Phytanic acid activates the peroxisome proliferator-activated receptor alpha (PPARalpha) in sterol carrier protein-2-/sterol carrier protein x-deficient mice. *J. Biol. Chem.* **274:** 2766–2772.
46. Hanhoff, T., S. Benjamin, T. Borchers, and F. Spener. 2005. Branched-chain fatty acids as activators of peroxisome proliferators. *Eur. J. Lipid Sci. Technol.* **107:** 716–729.
47. Hanhoff, T., C. Wolfrum, P. Ellinghaus, U. Seedorf, and F. Spener. 2001. Pristanic acid is activator of PPARalpha. *Eur. J. Lipid Sci. Technol.* **103:** 75–80.
48. Hara, A., and N. S. Radin. 1978. Lipid extraction of tissues with a low toxicity solvent. *Anal. Biochem.* **90:** 420–426.
49. Jefferson, J. R., J. P. Slotte, G. Nemecz, A. Pastuszyn, T. J. Scallen, and F. Schroeder. 1991. Intracellular sterol distribution in transfected mouse L-cell fibroblasts expressing rat liver fatty acid binding protein. *J. Biol. Chem.* **266:** 5486–5496.
50. Murphy, E. J., T. A. Rosenberger, and L. A. Horrocks. 1997. Effects of maturation on the phospholipid and phospholipid fatty acid compositions in primary rat cortical astrocyte cell cultures. *Neurochem. Res.* **22:** 1205–1213.
51. Bradford, M. M. 1976. A rapid and sensitive method for the quantitation of microgram quantities of protein utilizing the principle of protein dye binding. *Anal. Biochem.* **72:** 248–254.
52. Atshaves, B. P., H. R. Payne, A. L. McIntosh, S. E. Tichy, D. Russell, A. B. Kier, and F. Schroeder. 2004. Sexually dimorphic metabolism of branched chain lipids in C57BL/6J mice. *J. Lipid Res.* **45:** 812–830.
53. Mocking, R. J. T., J. Assies, A. Lok, H. G. Ruhe, M. W. J. Koeter, I. Visser, C. L. H. Bockting, and A. H. Schene. 2012. Statistical methodological issues in handling of fatty acid data: percentage or concentration, imputation, and indices. *Lipids.* **47:** 541–547.
54. Di Pietro, S. M., and J. A. Santome. 2000. Isolation, characterization, and binding properties of two rat liver fatty acid binding protein isoforms. *Biochim. Biophys. Acta.* **1478:** 186–200.
55. Maatman, R. G., H. T. van Moerkerk, I. M. Nooren, E. J. van Zoelen, and J. H. Veerkamp. 1994. Expression of human liver fatty acid-binding protein in Escherichia coli and comparative analysis of its binding characteristics with muscle fatty acid-binding protein. *Biochim. Biophys. Acta.* **1214:** 1–10.
56. Stolowich, N., A. Frolov, A. D. Petrescu, A. I. Scott, J. T. Billheimer, and F. Schroeder. 1999. Holo-sterol carrier protein-2: ^{13}C-NMR investigation of cholesterol and fatty acid binding sites. *J. Biol. Chem.* **274:** 35425–35433.
57. Avdulov, N. A., S. V. Chochina, U. Igbavboa, C. H. Warden, F. Schroeder, and W. G. Wood. 1999. Lipid binding to sterol carrier protein-2 is inhibited by ethanol. *Biochim. Biophys. Acta.* **1437:** 37–45.
58. Atshaves, B. P., G. G. Martin, H. A. Hostetler, A. L. McIntosh, A. B. Kier, and F. Schroeder. 2010. Liver fatty acid binding protein (L-FABP) and dietary obesity. *J. Nutr. Biochem.* **21:** 1015–1032.
59. Bordewick, U., M. Heese, T. Borchers, H. Robenek, and F. Spener. 1989. Compartmentation of hepatic fatty-acid-binding protein in liver cells and its effect on microsomal phosphatidic acid biosynthesis. *Biol. Chem. Hoppe Seyler.* **370:** 229–238.
60. Milligan, S., G. G. Martin, D. Landrock, A. L. McIntosh, J. T. Mackie, F. Schroeder, and A. B. Kier. 2017. Impact of dietary phytol on lipid metabolism in SCP2/SCPx/L-FABP null mice. *Biochim. Biophys. Acta.* **1862:** 291–304.
61. Landrock, D., S. Milligan, G. G. Martin, A. L. McIntosh, K. Landrock, F. Schroeder, and A. B. Kier. Effect of Fabp1/Scp-2/Scp-x ablation on whole body and hepatic phenotype of phytol-fed male mice. *Lipids.* Epub ahead of print. April 5, 2017; doi:10.1007/s11745-017-4249-y.
62. Wanders, R. J. A., J. Komen, and S. Ferdinandusse. 2011. Phytanic acid metabolism in health and disease. *Biochim. Biophys. Acta.* **1811:** 498–507.
63. Martin, G. G., B. P. Atshaves, A. L. McIntosh, J. T. Mackie, A. B. Kier, and F. Schroeder. 2008. Liver fatty acid binding protein gene-ablated female mice exhibit increased age-dependent obesity. *J. Nutr.* **138:** 1859–1865.
64. Murphy, E. J., D. R. Prows, J. R. Jefferson, and F. Schroeder. 1996. Liver fatty acid binding protein expression in transfected fibroblasts stimulates fatty acid uptake and metabolism. *Biochim. Biophys. Acta.* **1301:** 191–198.
65. Murphy, E. J. 1998. L-FABP and I-FABP expression increase NBD-stearate uptake and cytoplasmic diffusion in L-cells. *Am. J. Physiol.* **275:** G244–G249.
66. McArthur, M. J., B. P. Atshaves, A. Frolov, W. D. Foxworth, A. B. Kier, and F. Schroeder. 1999. Cellular uptake and intracellular trafficking of long chain fatty acids. *J. Lipid Res.* **40:** 1371–1383.
67. Murphy, E. J. 1998. Sterol carrier protein-2 expression increases fatty acid uptake and cytoplasmic diffusion in L-cell fibroblasts. *Am. J. Physiol.* **275:** G237–G243.
68. Murphy, E. J., and F. Schroeder. 1997. Sterol carrier protein-2 mediated cholesterol esterification in transfected L-cell fibroblasts. *Biochim. Biophys. Acta.* **1345:** 283–292.
69. Hostetler, H. A., D. Lupas, Y. Tan, J. Dai, M. S. Kelzer, G. G. Martin, G. Woldegiorgis, A. B. Kier, and F. Schroeder. 2011. Acyl-CoA binding proteins interact with the acyl-CoA binding domain of mitochondrial carnitine palmitoyltransferase I. *Mol. Cell. Biochem.* **355:** 135–148.
70. Hostetler, H. A., A. L. McIntosh, B. P. Atshaves, S. M. Storey, H. R. Payne, A. B. Kier, and F. Schroeder. 2009. Liver type fatty acid binding protein (L-FABP) interacts with peroxisome proliferator activated receptor-a in cultured primary hepatocytes. *J. Lipid Res.* **50:** 1663–1675.
71. Hostetler, H. A., M. Balanarasimha, H. Huang, M. S. Kelzer, A. Kaliappan, A. B. Kier, and F. Schroeder. 2010. Glucose regulates fatty acid binding protein interaction with lipids and PPARa. *J. Lipid Res.* **51:** 3103–3116.
72. Schroeder, F., A. D. Petrescu, H. Huang, B. P. Atshaves, A. L. McIntosh, G. G. Martin, H. A. Hostetler, A. Vespa, K. Landrock, D. Landrock, et al. 2008. Role of fatty acid binding proteins and long chain fatty acids in modulating nuclear receptors and gene transcription. *Lipids.* **43:** 1–17.
73. Gao, M., Y. Ma, and D. Liu. 2015. High-fat diet-induced adiposity, adipose inflammation, hepatic steatosis, and hyperinsulinemia in outbred CD-1 mice. *PLoS One.* **10:** e0119784.
74. Fengler, V. H. I., T. Macheiner, S. M. Kessler, B. Czepukojc, K. Gemperlein, R. Muller, A. K. Kiemer, C. Magnes, J. Haybaeck, C. Lackner, et al. 2016. Susceptibility of different mouse wild-type strains to develop diet induced NAFLD/AFLD associated liver disease. *PLoS One.* **11:** e0155163.
75. Fengler, V. H. I., T. Macheiner, and K. Sargsyan. 2016. Manifestation of NAFLD/NASH in different dietary mouse models. *Hepatology.* **4:** 94–102.
76. Adida, A., and F. Spener. 2002. Intracellular lipid binding proteins and nuclear receptors involved in branched-chain fatty acid signaling. *Prostaglandins Leukot. Essent. Fatty Acids.* **67:** 91–98.
77. Wolfrum, C., T. Borchers, J. C. Sacchettini, and F. Spener. 2000. Binding of fatty acids and perooxisome proliferators to orthologous fatty acid binding proteins from human, murine, and bovine liver. *Biochemistry.* **39:** 1469–1474.
78. McIntosh, A. L., H. Huang, S. M. Storey, K. Landrock, D. Landrock, A. D. Petrescu, S. Gupta, B. P. Atshaves, A. B. Kier, and F. Schroeder. 2014. Human FABP1 T94A variant impacts fatty acid metabolism and PPARa activation in cultured human female hepatocytes. *Am. J. Physiol. Gastrointest. Liver Physiol.* **307:** G164–G176.
79. Weisiger, R. A. 2002. Cytosolic fatty acid binding proteins catalyze two distinct steps in intracellular transport of their ligands. *Mol. Cell. Biochem.* **239:** 35–43.
80. Klipsic, D., D. Landrock, G. G. Martin, A. L. McIntosh, K. K. Landrock, J. T. Mackie, F. Schroeder, and A. B. Kier. 2015. Impact of SCP-2/SCP-x gene ablation and dietary cholesterol on hepatic lipid accumulation. *Am. J. Physiol. Gastrointest. Liver Physiol.* **309:** G387–G399.
81. Woldegiorgis, G., J. Bremer, and E. Shrago. 1985. Substrate inhibition of carnitine palmitoyltransferase by palmitoyl-CoA and

activation by phospholipids and proteins. *Biochim. Biophys. Acta.* **837:** 135–140.
82. Seedorf, U., P. Brysch, T. Engel, K. Schrage, and G. Assmann. 1994. Sterol carrier protein X is peroxisomal 3-oxoacyl coenzyme A thiolase with intrinsic sterol carrier and lipid transfer activity. *J. Biol. Chem.* **269:** 21277–21283.
83. Kannenberg, F., P. Ellinghaus, G. Assmann, and U. Seedorf. 1999. Aberrant oxidation of the cholesterol side chain in bile acid synthesis of sterol carrier protein-2/sterol carrier protein-x knockout mice. *J. Biol. Chem.* **274:** 35455–35460.
84. Mönnig, G., J. Wiekowski, P. Kirchhof, J. Stypmann, G. Plenz, L. Fabritz, H-J. Bruns, L. Eckardt, G. Assmann, W. Haverkamp, et al. 2004. Phytanic acid accumulation is associated with conduction delay and sudden cardiac death in sterol carrier protein-2/sterol carrier protein-x deficient mice. *J. Cardiovasc. Electrophysiol.* **15:** 1310–1316.
85. Yoon, M. 2009. The role of PPARa in lipid metabolism and obesity: focusing on the effects of estrogen on PPARa actions. *Pharmacol. Res.* **60:** 151–159.
86. Murphy, E. J., R. D. Edmondson, D. H. Russell, S. M. Colles, and F. Schroeder. 1999. Isolation and characterization of two distinct forms of liver fatty acid binding protein from the rat. *Biochim. Biophys. Acta.* **1436:** 413–425.
87. Richieri, G. V., R. T. Ogata, and A. M. Kleinfeld. 1994. Equilibrium constants for the binding of fatty acids with fatty acid binding proteins from adipocyte, intestine, heart, and liver measured with the fluorescent probe ADIFAB. *J. Biol. Chem.* **269:** 23918–23930.
88. Schroeder, F., C. A. Jolly, T. H. Cho, and A. A. Frolov. 1998. Fatty acid binding protein isoforms: structure and function. *Chem. Phys. Lipids.* **92:** 1–25.